Published in final edited form as:
J Chem Inf Model. 2013 June 24; 53(6): 1424–1435. doi:10.1021/ci400112k.

Structural Determinants of Drug Partitioning in n-Hexadecane/Water System

Senthil Natesan[a], **Zhanbin Wang**[a], **Viera Lukacova**[b,c], **Ming Peng**[b], **Rajesh Subramaniam**[a], **Sandra Lynch**[a], and **Stefan Balaz**[a,*]

[a]Department of Pharmaceutical Sciences, Albany College of Pharmacy and Health Sciences, Vermont Campus, Colchester, VT, United States

[b]College of Pharmacy, North Dakota State University, Fargo, North Dakota 58012, United States

Abstract

Surrogate phases have been widely used as correlates for modeling transport and partitioning of drugs in biological systems, taking advantage of chemical similarity between the surrogate and the phospholipid bilayer as the elementary unit of biological phases, which is responsible for most of transport and partitioning. Solvation in strata of the phospholipid bilayer is an important drug characteristics because it affects the rates of absorption and distribution, as well as the interactions with the membrane proteins having the binding sites located inside the bilayer. The bilayer core can be emulated by n-hexadecane (C16), and the headgroup stratum is often considered a hydrophilic phase because of the high water content. Therefore, we tested the hypothesis that the C16/water partition coefficients (*P*) can predict the bilayer locations of drugs and other small molecules better than other surrogate systems. Altogether 514 $P_{C16/W}$ values for nonionizable (458) and completely ionized (56) compounds were collected from the literature or measured, when necessary. With the intent to create a fragment-based prediction system, the $P_{C16/W}$ values were factorized into the fragment solvation parameters (*f*) and correction factors based on the ClogP fragmentation scheme. A script for the $P_{C16/W}$ prediction using the ClogP output is provided. To further expand the prediction system and reveal solvation differences, the $f_{C16/W}$ values were correlated with their more widely available counterparts for the 1-octanol/water system (O/W) using solvatochromic parameters. The analysis for 50 compounds with known bilayer location shows that the available and predicted $P_{C16/W}$ and $P_{O/W}$ values alone or the $P_{C16/O}$ values representing their ratio do not satisfactorily predict the preference for drug accumulation in bilayer strata. These observations indicate that the headgroups stratum, albeit well hydrated, does not have solvation characteristics similar to water and is also poorly described by the O/W partition characteristics.

INTRODUCTION

The use of surrogate phases in drug-related research is based on the linear relationship[1] between the logarithms of the partition coefficients in two two-phase systems, consisting of similar phases, with the slope and intercept obtained from a correlation with experimental data and determined by the phases and experimental conditions. Similarity in this context means the ability of the molecules of the two phases to form similar interactions with the drug molecules. The surrogate systems are not used with the aim to obtain an exact magnitude of a solvation-related biological property. Rather, they are meant to provide a

*Corresponding author: stefan.balaz@acphs.edu, +1-802-735-2615.
[c]Simulation-Plus, Inc., Lancaster, California 93534, United States.

correlate – a parameter that can be used to calculate the biological characteristics via the Collander equation.

The most widely used surrogate phase is wet 1-octanol,[2] which mimics phospholipid bilayer in biological membranes. At room temperature and normal pressure, wet 1-octanol contains 2.5 mol/L of water,[3] which represents molar fraction[4] of 0.26 and volume fraction[5] of about 0.04. An analysis of X-ray diffraction patterns showed that 1-octanol molecules form fluctuating inverted micellar aggregates, with water present around the arrangements of hydroxyl groups, whereby the alkyl chains point out in almost extended conformations.[6] There is some controversy about the shape of the hydroxy group aggregates and their interaction with water. The X-ray[6] and ^{1}H NMR data[7] point to nearly spheric arrangements of the hydroxyls. Molecular dynamics simulations[8] result in linear networked chains of H-bonded hydroxyls, which look like remnants of those seen by X-ray crystallography[9] at 150K. Spectroscopic data indicate that water in saturated 1-octanol does not disturb the H-bonding of 1-octanol molecules present in neat 1-octanol and forms pockets maintaining a similar structure as bulk water in the proximity of hydroxyls.[4] The biphasic microstructure of wet 1-octanol allows partitioning of the nonpolar compounds into the alkyl chain regions and interactions of H-bonding solutes with water and hydroxyl groups, as indicated by ^{1}H NMR data[7] and molecular dynamics simulations.[10] In this way, wet 1-octanol imitates, to some extent, overall partitioning of drugs between phospholipid bilayers and surrounding water.

Rather than the overall partitioning, separate drug affinities for the headgroup and core strata of the bilayer are required for quantitative understanding of several key processes in drug action. They include transbilayer permeation and bilayer accumulation,[11] as well as drug interactions with membrane-bound proteins, including efflux pumps,[12] cytochromes P450,[13] as well as cyclooxygenases[14] and possibly other therapeutically important targets, which have the (entry to) drug binding sites located inside the bilayer.

The solvation properties of the bilayer core can be, thanks to similar densities and composition,[15] emulated by n-hexadecane (C16)[16] or other alkane/alkene, such as 2,4,4-trimethylpentane,[17] n-hexane,[18] n-heptane,[19] isooctane,[20] n-decane,[21] n-dodecane,[22] 1-hexadecene, 1,9-decadiene,[21] or loosely defined alkane mixtures.[23] The partition coefficients of compounds in different alkane/water systems have quite similar magnitudes.

The differences ($\Delta \log P$) between the partition coefficients in the 1-octanol/water system and in the cyclohexane/water,[24] alkane/water,[25] isooctane/water,[20] dodecane/water or C16/water[22] systems were used as correlates for transport through the blood/brain barrier. The fraction absorbed in human was shown to depend on the $\Delta \log P$ values for the alkane/water system.[26] These studies indicate the usefulness of the alkane/water systems in describing drug distribution. We focus on a different aspect of the distribution problem: the prediction of bilayer location of drugs.

Taking into account that, depending on the area per phospholipid, temperature and pressure, there are 6-16 molecules of water per a headgroup[27-29] in phosphatidylcholine bilayer and neglecting the hydration interactions decreasing the available water concentration, several computational studies[30-34] treated the headgroups as an aqueous phase. If this assumption holds, the C16/water partition coefficient should be a good predictor of the bilayer location. We wanted to test this hypothesis.

As a headgroup surrogate, water-immiscible solvents with the molecules containing some phospholipid fragments – isopropyl myristate,[35] propylene glycol dipelargonate,[36] and n-butyl acetate[37] – were used in combination with water. The values of these partition coefficients can be used as denominators in the ratios with those of the respective alkane/

water partition coefficients to reveal the H-bonding properties of the compounds, as it was done with 1-octanol.[38]

These surrogate phases differ in composition from phospholipid headgroups: they lack the phosphate and other charged groups, and some contain additional H-bond donors, which are not found in the headgroups. None of the mentioned surrogate phases can, therefore, fully emulate all drug interactions with the headgroups. A straightforward solution to this problem is the use of properly hydrated diacetyl phosphatidylcholine (DAcPC) – the diacetylated headgroup of the prevalent mammal phospholipid - as a surrogate phase for the headgroup region, as we suggested.[39] Hydrated DAcPC contains similar amounts of water as the headgroup region of fluid phospholipid bilayer, is only slightly viscous, and immiscible with n-hexadecane (C16) or other alkanes. The C16/DAcPC partition coefficients are, in combination with the C16/W partition coefficients, a good predictor of bilayer location of drugs.[39]

Other solvents, which bear no obvious structural resemblance to the headgroups or the core components (e.g., chloroform, benzene,[40] and ether[41]), were tested as two-phase systems with water to provide correlates of biological disposition. Ethylene glycol was used in a two-phase system with n-heptane to model transport of peptides across epithelial cell monolayers.[42] A different group of water-immiscible solvents imitates the structures of triglycerides rather than those of phospholipids. They include loosely defined oils of plant or animal origin and triolein.[43] Vegetable oil was used to imitate solvation properties of fat and phospholipids represented by a mixture of 30% lipids and 70% water.[44-46]

The C16/water (C16/W) partition coefficients, or alkane/water partition coefficients in general, represent an important component of any surrogate system aiming at the understanding of drug affinities for headgroups and cores. As compared with widely used methods for estimation of the 1-octanol /water (O/W) partition coefficients from drug structure,[47] published methods for the C16/W partition coefficients[21;26;48-50] are less available. With the present study, we want to expand the tool set for numerous ClogP users by generating the ClogP parameters[51] for the C16/W partitioning using a carefully selected set of measured and published C16/W partition coefficients. To focus on a well-defined system and increase the precision of the estimates, we refrained from the indiscriminate use of the partition coefficients measured with loosely defined alkane mixtures and those for partially ionized compounds. The calibrated C16/W fragment system will facilitate the analysis of solvation differences between the wet C16 and O phases. The predicted values of the C16/W partition coefficient will be tested for the ability to predict bilayer location of the compounds, for which this information is available.

MATERIALS AND METHODS

Materials

The compounds were purchased from Sigma-Aldrich and n-hexadecane (99%) was purchased from Alfa Aesar. Water was purified by Thermo Barnstead Nanopure® Ultrapure Water Systems.

Measurement of Partition Coefficients

The C16/W partition coefficients of 25compounds (Table 1) were measured by the shake-flask method. The used C16 and water phases mutually saturated through overnight contact in the incubator at 25 °C with the constant shaking rate of 25 rpm. The compound was usually dissolved in the C16 phase, and 1 mL of the solution was carefully layered on an appropriate volume (1 – 100 mL) of the aqueous phase in an appropriate glass container. The C16/W volume ratio was estimated in preliminary experiments, so that the final drug

concentration in the C16 phase would reach 5-95% of the initial concentration. For each partitioning experiment, five samples along with five corresponding controls were placed in the incubator at 25 °C shaking at 25 rpm. The samples were withdrawn at appropriate intervals ranging from 0 to 48 hrs. At each sampling time, the drug concentrations in both C16 and water phases, where feasible, were determined by UV/Vis spectroscopy. For all measured compounds, the equilibrium was reached or was approaching within the timescale of the experiment. Two-compartment kinetic models were used to ensure that the equilibrium conditions were estimated as closely as feasible. The time course of the concentration c in the C16 phase can be described as

$$c_{C16}(t) = \frac{c_{C16}(0)}{l_1 V_{C16} + l_2 V_W}\left[l_2 V_W e^{-\left(\frac{Al_1}{V_W} + \frac{Al_2}{V_{C16}}\right)t} + l_1 V_{C16}\right] \quad (1)$$

Here l_1 and l_2 are the rate parameters of transport from water to C16 and backwards, respectively; V is the volume of the phase indicated in the subscript, A is the surface area of the interface, and t is time. The corresponding aqueous concentration can be described as

$$c_W(t) = \frac{c_{C16}(0)\, l_2 V_{C16}}{l_1 V_{C16} + l_2 V_W}\left[1 - e^{-\left(\frac{Al_1}{V_W} + \frac{Al_2}{V_{C16}}\right)t}\right] \quad (2)$$

The rate parameters and their errors were determined by the fit of eqs 1 and 2 to experimental data.[52] The partition coefficient was calculated as $P = l_1/l_2$, with the error given by

$$\delta P = |P| \sqrt{(\delta l_1/l_1)^2 + (\delta l_2/l_2)^2} \quad (3)$$

Here, δl_1 and δl_2 are the errors of the transport rate parameters l_1 and l_2, respectively.

Used Data

The C16/W partition coefficients for 460 compounds were collected from literature.[18;38;53-67] To expand the pool, 145 alkane/water (A/W) partition coefficients were also collected[18;38;53-61;64;65] and used to predict the C16/W partition coefficients for additional 208 compounds. All used data are listed in Table S1 in Supporting Information.

Linear Regression Analyses

The correlation equation 5 (shown later) was used, with the fragments generated by the ClogP program.[68] The linear regression analyses[52;69] were performed in a step-wise manner, starting with the compounds composed of only C and H atoms initially and gradually adding compounds with less frequently occurring fragments, to check for additivity of the fragment solvation characteristics and stability of the system.

Script for Using ClogP Output to Predict the C16/W Partition Coefficients

A Perl executable is available through a link on our laboratory web site (http://www.acphs.edu/Academics/Profiles/DepartmentOfPharmaceuticalSciences/BalazLab/Research_Overview.aspx). The script can be run on any operating system with no additional software requirements. A library file with the fragments and correction factors values provided along with the executable should be present in the same directory. The primary input for the program is the detailed output from ClogP program. Additional information is contained in the accompanying text file. After successful execution of the script, a detailed text output with predicted $\log P_{C16/W}$ values of given compounds is produced.

RESULTS AND DISCUSSION

Measured n-Hexadecane/Water Partition Data

Partitioning of 25compounds in the C16/W system was monitored experimentally at 25 °C, to expand the data set of published values for the estimation of fragment solvation parameters and correction factors and include some of the more rare fragments. The kinetics of the process was monitored to ensure that the equilibrium partitioning was attained. The results are summarized in Table 1.

For the partition coefficients, which are measured under identical conditions for all compounds, in the same vessel and using the same stirring rates, the transport rate parameters l_1 and l_2 for transport from the aqueous phase to the nonpolar phase and backwards, respectively, depend on the partition coefficient P:[70]

$$l_1=\frac{\alpha P}{\beta P+1} \quad \text{and} \quad l_2=\frac{\alpha}{\beta P+1} \quad (4)$$

The optimized parameters α and β are constant for the given hydrodynamics of the two phase systems. The fits to experimental data are usually excellent, explaining more than 95% of the variance in the data.[70] They hold for compounds of different structures, for ionizable molecules and ion pairs,[71] and even when measured at different pH values if the distribution coefficients are used.[63] For these reasons, eqs 4 are frequently used in simulations of drug transport in a series of aqueous and nonpolar phases.[72] In our experiments, different volumes of the phases were used that could not be accommodated in identical vessels. Different hydrodynamics affects the transport rates because it determines the thickness of the unstirred diffusion layers at the interface. Therefore, our data (Table 1) do not conform to eqs 4, although the trends are similar.

Used Data

Altogether 460 values of the C16/W partition coefficient were collected from literature. Alkane/water (A/W) partition coefficients are often pooled together for the correlations with the biological characteristics because the differences in their magnitudes are small. To further narrow the scatter, the C16/W partition coefficients were re-scaled from reliable A/W values. The fit for the C16/W partition coefficients as the dependent variable, with both variables logarithmized, is characterized by the slope of 1.006, the intercept of −0.063, and the following statistical indices: the number of points, n = 145, the squared correlation coefficient, r^2=0.992, and the standard deviation, SD =0.158 ($p < 0.0001$). This correlation was used to predict the C16/W partition coefficient for additional 208 compounds. With our 25 measured values, the total number of used compounds was 693. All data are included in Table S1 in Supporting Information.

All used $\log P_{C16/W}$ values are plotted against the $\log P_{O/W}$ values in Figure 1. For most compounds, the $P_{C16/W}$ values are lower than the $P_{O/W}$ values, reflecting the fact that, in the latter system, H-bonds can be formed in both phases. Some small molecules (carbon oxide, dimethyl sulfoxide, hydrogen, nitrogen, and nitrous oxide, plotted as crosses in Figure 1) exhibit higher affinity for n-hexadecane than for 1-octanol. However, this trend is not observed for carbon dioxide, oxygen, and water.

Could the high water content in wet 1-octanol result in a limit on the minimum $P_{O/W}$ values for compounds that can be fully hydrated in the water present in wet 1-octanol? The water-OH clusters of wet 1-octanol contain ~30 or 40 oxygen atoms.[8;10] The opinions about the shape of these clusters differ: spectroscopic evidence points to water aggregates of close-to-spherical shape[7] where the H-bonds between water molecules are preferred to those with the

OH-groups of 1-octanol,[4] while molecular dynamics simulations[8] indicate that water molecules are spread along the chains of H-bonded OH-groups forming a prolate ellipsoid shape of the aggregate. The former situation would lead to a better accommodation of most dissolved molecules of hydrophilic compounds. If all 4% vol. of water in saturated 1-octanol would participate in hydration of compounds, the concentration of the compound in the microheterogeneous 1-octanol phase could be estimated as $0.04\times c_W + 0.96\times c_N$ (N indicating nonpolar regions formed by alkyl chains of 1-octanol). For very hydrophilic compounds, c_N would approach zero resulting in the minimum $P_{O/W} \sim 0.04$. The line in Figure 1 is described by logarithmized equation $P_{C16/W}=(P_{O/W}-0.04)/0.96$, which corresponds to this hypothesis. Many $P_{O/W}$ values have been reported that are lower than the limit of 0.04, especially for charged molecules. Obviously, the limit $P_{O/W}$ value would only hold for smaller molecules, which could be fully hydrated in the water-OH clusters of the 1-octanol phase. In addition, the measurement of extreme P values is difficult and prone to artifacts. While special methods have been developed for the measurement of the high log$P$ values,[73] no such developments can be found for the low log$P$ values.

Fragment Solvation Parameters and Correction Factors

The ClogP fragmentation scheme[51] was chosen because of its sound physicochemical basis. The scheme uses isolating carbons to define fragments of interacting atoms, which are treated as separate units. Although this idea could not be applied rigorously for statistical reasons and aromatic carbons had to be added to the category of isolating carbons, the approach still allows a meaningful analysis of structural determinants of solvation and their comparison between different systems. The original O/W ClogP fragment solvation characteristics were optimized in a 'constructionist' sense, starting with the simplest molecules and gradually adding more complex molecules.

Ionization complicates evaluation of the partition experiments because of the presence of several molecular species, which have different solvation energies in the used phases. To reduce the multiplicity of species, 41 ionizable compounds with the pK_a values between 5 and 9 (Table S1 in Supplementary information) were excluded from the data set. The values for 56 ionizable compounds with the pK_a values outside this interval, which are practically completely ionized for pH ~ 7, were used in the analyses.

The resulting 652 compounds were subjected to the fragmentation by the ClogP program. Unfortunately, 126 compounds contained fragments or correction factors, which did not reach, in all studied compounds, the count of 3 that was set as a minimum for inclusion into the analyses.

Altogether 526 published (360), re-scaled (147), and measured (19) values of the C16/W partition coefficients (Table S1 in Supporting Information) were correlated with structure using the ClogP approach:[51]

$$\log P_{C16/W} = \sum_i a_i f_i + \sum_j b_j F_j \quad (5)$$

where f are fragment solvation parameters for fragments occurring with frequency a in the given molecule and F are the correction factors having frequencies b.

In the ClogP system, some of the factors are treated in a complex way, utilizing fragment-specific parameters, different from f, which could not be completely calibrated using our limited data set. We had to simply collapse to a single value several factors, which are represented in the ClogP system by multiple values: Hydrogen Bonding (HB), Interacting Fragments (InterFrag), Ether in Five-Member Ring (O5R), Pair Proximity (Proximity), and

Y-fragment (Yfragment). The shortage of data made us to take a simplified binning approach to Potential Interaction within Ring (PIWR), and Normal Ortho (Northo) and Proximity (NOprox) factors.

The PIWR factor describes the interaction between two substituents on an aromatic ring, which leads to a decrease in hydration of these substituents, and consequently to positive PIWR values spanning almost one log unit (0.076 to 0.954) in the ClogP outputs for our data set, depending upon the substituent groups. The substituent interaction can be considered bidirectional. Each substituent was assigned a σ value as an inducer, and a ρ value as a responder, which are specific for the ClogP system.[74] Higher σ (for electron withdrawing groups, e.g., NO_2 and CN) and ρ values (for electron donating groups, e.g., OH and NH_2) result in a higher PIWR correction factor. These characteristics are associated with overall hydration of fragments and exhibit similar trends as the fragment solvation parameters, *f*. Our data set would not allow a reasonable optimization of the σ and ρ values, so we decided to use three different magnitudes of the PIWR correction factor. The PIWR1 has the lowest value and is applied to the interaction of the fragments with the ClogP fragment values, *f*, lower than 0.15. The intermediate PIWR2 describes the interaction of the fragments with $0.15 \leq f \leq 0.5$, which represent a combination of a strong inducer and weak responder or vice versa. The highest PIWR3 value is attributed to the presence of strong H-bond accepting inducers and strong responders with H-bond donating ability, which is generally associated with $f > 0.5$.

The ortho interaction modifies formation of the hydration shell around two interacting fragments from the extent that is represented by the sum of the hydration shells of separated fragments. The ClogP system uses specific parameters for each fragment involved in an ortho interaction. The size of our data set does not allow the optimization of all involved parameters. Therefore, we optimized three different NOrtho correction factors according to the following classification. The NOrtho1 is used if one of the interacting group is isolated aromatic or aliphatic carbon (ClogP fragment values $f > -0.12$). The NOrtho2 is applied if both interacting groups are halogens, essentially based on the values of $-0.25 \leq f \leq -0.12$. The NOrtho3 correction factor is used for all other fragments ($f < -0.25$). If the interacting fragments have the *f* values from different categories, an average NOrtho or PIWR value would be a natural choice, although our data did not provide for testing of this approach.

The step-wise regression analyses (Table S2 in Supporting Information) showed that the correlations were stable and the contributions of individual solvation parameters (*f*) and correction factors (*F*) can be treated as additive. To keep the values of optimized coefficient as precise as possible, 12 compounds with the predicted $\log P_{C16/W}$ values differing by more than 1 unit from the experimental values were excluded as outliers (Table S1 in Supporting Information) because of possible experimental errors or problems with our approximate treatment of some correction factors. For the final correlation, the statistical indices were n = 514, $r^2 = 0.987$, and SD = 0.240. The optimized *f* and *F* values are summarized in Tables 2 and 3, respectively, along with their standard error and the counts in which they occur in the data set. The ClogP counterparts are listed for comparison.

Almost all fragment solvation parameters, *f*, in the C16/W and O/W systems (Table 2) have the same sign and only differ in the magnitudes. The only exceptions are the aliphatic chlorine substituent (ClA, **6**) and the oxygen in an aromatic ring (Oxgenaa, **19**). The ClA parameter is of a small magnitude, and takes a positive value in the O/W system, while being negative in the C16/W systems. The Oxgenaa parameters have larger absolute values and have the signs changed in the opposite direction. A similar fragment, the ether oxygen flanked by two aromates (Oaa, **17**), has a positive value in both systems, probably because of efficient conjugation of the oxygen electron pairs with the π-electrons of the aromates.

A similar situation is seen among the correction factors (Table 3), where the exceptions are the NOrtho1 (**65**) and XBenzyl (**75**) factors. The NOrtho1 factor is positive in the C16/W system, although equivalent factors are slightly negative in the ClogP system (not shown). This factor describes the ortho interaction of two aliphatic or aromatic carbons, which diminishes hydrophobic/dispersion hydration shell when the substituents are in the ortho contact, as compared with the shell for the carbons in independent positions. Therefore, a negative value would be expected for the NOrtho1 effect. Apparently, there are additional influences at play because the fitted positive NOrtho1 value of 0.147±0.058 is quite conclusive: the error is about 40% and the factor is encountered in 24 compounds. The XBenzyl factor is used in 4 compounds and is also positive in the C16/W system while it takes several slightly negative values in the O/W system.

To reveal quantitative contributions of solute properties to the differences between the C16/W and O/W (ClogP) fragment solvation parameters, their values can be correlated using the solvatochromic equation [53] as

$$f_{\mathrm{C16/W}} = f_{\mathrm{ClogP}} + e \times E + s \times S + a \times A + b \times B + v \times V + const \quad (6)$$

where E is the excess molar refraction, S is dipolarity/polarizability, A is overall H-bond acidity, B is the overall H-bond basicity, and V is the characteristic volume. These properties can be used to describe the C16/W and O/W fragment sets separately. Therefore, the property terms in eq 6 represent the differences between the two fragment sets. Solvatochromic properties have been defined for intact molecules, so they need to be estimated for fragments. Fragment contributions to solvatochromic properties of molecules have been analyzed[75] but some of the published values were not consistent with the expected properties of fragments. Therefore, we decided to estimate the solvatochormic properties for fragments attached to alkyls using the experimental values of suitable alkyl derivatives. Excess molar refraction (E) and characteristic volume (V) are additive properties, so we used their experimental values for methyl and ethyl derivatives, or those of 5- and 6-membered aliphatic rings for ring fragments, to extrapolate to the values for the fragments. For dipolarity/polarizability (S), H-bond acidity (A) and H-bond basicity (B), the values in alkyl series level off at ethyls in the vast majority of cases, so the experimental values of ethyl derivatives were used directly as the estimates of these properties. The estimated solvatochromic contributions of fragments attached to alkyls are summarized in Table 2. The A and B values for alkyl-attached fragments were identical with the published H-bond structural constants,[76] so these values for fragments attached to aromates are also listed in Table 2.

Linear regression analysis of the data in Table 2 using eq 6 showed that the *e, v*, and *const* terms have the errors larger than the values themselves and do not contribute to the correlation. When these values were set to zero, the remaining values were optimized as follows: $s = -0.487 \pm 0.245$, $a = -3.196 \pm 0.465$, and $b = -1.660 \pm 0.287$. The statistical indices were n=24, $r^2 = 0.962$, and SD = 0.131. If only the dominant H-bonding terms are considered, the fragments attached to aromates can also be included. The correlation is then characterized by the optimized coefficients values $a = -3.434 \pm 0.479$ and $b = -2.112 \pm 0.187$, and the statistical indices n = 40, $r^2 = 0.955$, and SD=0.148. The optimized coefficient values are in good agreement with the values obtained for the difference $\log P_{\mathrm{O/W}} - \log P_{\mathrm{C16/W}}$ (i.e., the terms have the opposite signs to those in eq 6) for 288 molecules:[53] $s = 0.522$, $a = 3.877$ and $b = 1.591$, with low magnitudes of coefficients e and *const*. This study also found that the volume term was important ($v = -0.407$), in contrast to our correlation, where this term has the largest error. Instead, the s term was significant in our correlation. The S and V contributions have the highest cross-correlation in our data ($r^2 = 0.590$), all other r^2 values are below 0.288.

The C16/W and O/W fragment solvation parameters were compared in Figure 2, taking into account their H-bonding ability, which is the main cause of the difference in solvation in these two systems.[38] To classify the H-bonding ability of individual fragments, H-bond structural constants A and B were used[76] (Table 2). For robust characterization, the thresholds for H-bond acidity and basicity were set at 0.16. Under these conditions, some weak H-bond acceptors, such as aliphatic and aromatic halogens (**4**-**12**, Table 2), thiophene sulfur (**13**), and trifluoromethyl substituent (**35**), were classified as having no H-bonding ability. To expand the H-bonding classification, some extrapolations were used for the fragments with missing H-bond structural constants. The basicity constant (B) of ether oxygen fell sharply almost to our limit (0.16), when one of the two attached alkyls (**15**) was replaced by an aromate (**16**). Consequently, the oxygens flanked by two aromatic systems (**17**) and inside an aromatic ring (**19**) but not in an aliphatic ring (**18**) were considered as having no H-bond acceptor ability. N-oxide (**20**) was considered as H-bond acceptor because the B value for the aromatic nitro group (**22**) was only slightly below the limit of 0.16. The benzyl hydroxyl (OHZ, **26**) was classified as H-bond donor and acceptor because the A and B values of both aliphatic (OHA, **25**) and aromatic (OHa, **27**) hydroxyls were above the limit of 0.16. The NH group in aromatic ring (NHaa, **31**), as well as the nitrogens in the aliphatic (NARR, **33**) and aromatic (Naraa, **34**) rings were considered as H-bond acceptors because the aliphatic secondary (NHAA, **30**) and tertiary (NAAA, **32**) amines have high H-bond basicities. A modest decrease in the H-bond basicity upon substitution of one of the two alkyls flanking a carbonyl (COAA, **36**) by an aromate (COAa, **38**) led to the classification of all carbonyls (including CORW, **37**, and COaa, **39**) as H-bond acceptors. Finally, the carbamate with the N in an aliphatic ring connected to aromate (CBMTRRa, **51**) was considered H-bond acceptor because the carbamate connected to an aromatic and an aliphatic residue (CBMTAa, **50**) is an H-bond donor and acceptor of intermediate strength, and **51** contains no hydrogen.

Using this classification, the ClogP and C16/W fragment parameters were plotted in Figure 2. Weak or missing H-bonding ability (fragments **1**-**13**, **17**, **19**, **22**, and **35** in Table 2) is associated with positive or only slightly negative fragment values, which have similar magnitudes in both C16/W and O/W systems (black points in Figure 2 positioned close to the identity line). More extensive H-bonding leads, in the vast majority of cases (except **24** and **43**), to more negative fragment values in both systems but the decrease is more pronounced for the C16/W system than for the O/W system. The differences are larger for H-bond donors/acceptors (**25**-**29**, **46**-**50**) than for H-bond acceptors (**14**-**16**, **18**, **20**, **21**, **23**, **24**, **30**-**34**, **36**-**45**, and **51**).

The fragment solvation parameter values are closely associated with the character of the two systems. Wet 1-octanol contains a significant amount of water located in the proximity of hydroxy groups. The biphasic structure gives the wet 1-octanol phase the ability to interact with H-bonding fragments in the water-hydroxyl aggregates, while nonpolar fragments are accommodated in the alkyl regions. Therefore, the addition of an H-bonding fragment to a solute molecule will increase the solute concentration in both 1-octanol and aqueous phases, the latter usually to a larger extent. The result is an overall decrease of the O/W partition coefficient. The decrease in the magnitude of the C16/W partition coefficient is much larger because the concentration of the solute in the n-hexadecane phase will decrease, as opposed to its increase in the aqueous phase.

Prediction of Bilayer Location

The biphasic nature of the wet 1-octanol imitates, to some extent, the biphasic structure of a phospholipid bilayer. For this reason the O/W partition coefficients emulate, to some extent, the bilayer/water partition coefficients according to the Collander equation,[1] especially for

uncharged solutes. As a consequence, the O/W partition coefficients are often the parameters of choice for the description of overall bilayer/water equilibria. For quantitative models of several key steps in drug pharmacokinetics, however, the drug concentrations in headgroup and core strata, and at the interface between them are of interest. These processes include the transbilayer transport,[11] and drug effects on membrane proteins such as P-glycoprotein,[12] cytochrome P450,[13] and several receptors, which have the drug-binding sites located inside the bilayer.

The headgroups are well hydrated[27-29] and were regarded as aqueous phases in several computational studies.[30-34] Then the C16/W partition coefficients, which are expected to provide the information about the drug affinity for the hydrophobic core of the bilayer, could be the only determinant of drug preference for individual bilayer strata. Can they be used to estimate the prevalent drug location in the biphasic bilayer? To answer this question, the data for 50 compounds with experimentally confirmed bilayer location in either headgroup stratum or in the core,[72] for which the C16/W partition coefficient were available or could be predicted using the solvation parameters (Table 2) and corrections factors (Table 3) obtained in this study were summarized in Tables 4-6, along with the O/W partition coefficients. Five lipophilic compounds (β-carotene, canthaxanthin, lutein, squalene, and zeaxanthin), although known to accumulate in the core,[72] were not listed because their predicted log*P* values were too high to be considered reliable. At least one but mostly both $\log P_{C16/W}$ and $\log P_{O/W}$ were larger than 9, and the uncertainties would affect the estimates of the C16/O (i.e., $P_{C16/W}/P_{O/W}$) partition coefficients. The $P_{C16/O}$ values characterize H-bonding ability of the compounds and provided good descriptions of transmembrane transport for some compounds.[25]

A good predictor of bilayer location would clearly separate the cephalophiles locating in the headgroups (Table 4) from the core-bound lipophiles (Table 6), ideally with some gap for compounds, which have a more balanced headgroup-core distribution. The data for amphiphiles with the headgroup/core interface are collected in Table 5. The locations are plotted against the C16/W, O/W, and C16/O partition coefficients in Figure 3.

The C16/W partition coefficients are larger than 1 for all lipophiles but also for many cephalophiles and amphiphiles (Figure 3, the top panel). For the O/W partition coefficients, the overlaps are large for all three types of bilayer location (the middle panel). All amphiphiles have the O/W and C16/O partition coefficients above 0.88 and below −0.92, respectively, in accord with the need for H-bonding in the headgroups. No efficient separation of cephalophiles and lipophiles was observed even for the C16/O partition coefficient (Figure 3, the bottom plot). There is no gap between lipophiles and other compounds. In fact, in the interval $-0.3 \le \log P\text{C16/O} \le 0.3$, compounds belonging to the two groups are freely mixing. In addition, there are several clearly wrong predictions: the cephalophiles 1-chloro-1,2,2-trifluoro-cyclobutane (compound **1** in Table 4), N-methylcarbazole (**15**), N-methylindole (**16**) have positive $\log P_{C16/O}$ values > 0.7, and lipophiles 4-bromo-2,6-*t*-butyl-phenol (compound **38** in Table 6), amiodarone (**42**) and benzocaine (**44**) exhibit negative $\log P_{C16/O}$ values lower than −0.8.

None of the examined partition coefficients provides a clear clue for location of a compound in the bilayer. This goal can be achieved using the C16/DAcPC partition coefficients,[39] in combination with the $P_{C16/W}$ values. The presented ClogP fragment solvation parameters (Table 2) and correction factors (Table 3) for the C16/W system make this task easier.

CONCLUSIONS

The study presents a consistent parametrization of the structure-based prediction system based on the ClogP fragmentation for partitioning in the C16/W system at 25 °C, using 514 published, extrapolated (from the A/W system), and measured values. Altogether, 51 fragment solvation parameters and 25 correction factors are provided, albeit with some approximations in the latter group. The errors of individual parameters were characterized, allowing for calculation of the error for structure-based estimates. The differences between the C16/W and O/W fragment solvation parameters were correlated with solvatochromic properties dipolarity/polarizability (*S*), and H-bond acidity (*A*) and basicity (*B*). The primary factor responsible for the differences is H-bonding, explaining 95% of variance. The correlations with solvatochromic parameters allow estimation of the unknown C16/W fragment solvation parameters using their ClogP counterparts. The measured and estimated C16/W partition coefficients of 50 compounds were compared with their experimentally determined bilayer location. The C16/W partition coefficients and their O/W counterparts alone or as ratios ($P_{C16/O}$) do not provide satisfactory prediction of preferred location of a drug in the bilayer regions. This observations indicate that (1) the headgroup stratum cannot be treated as an aqueous phase and (2) the $P_{C16/O}$ partition coefficients which describe H-bonding do not describe the interaction of drugs with the phospholipid headgroups.

Supplementary Material

Refer to Web version on PubMed Central for supplementary material.

Acknowledgments

This work was supported in part by the NIH NIGMS grant R01 GM80508.

REFERENCES

1. Collander R. Lipoid solubility. Acta Physiol. Scand. 1947; 13:363–381. [PubMed: 20273351]
2. Hansch C, Maloney PP, Fujita T, Muir RM. Correlation of biological activity of phenoxyacetic acids with Hammett substituent constants and partition coefficients. Nature. 1962; 194:178–180.
3. Dallas AJ, Carr PW. A thermodynamic and solvatochromic investigation of the effect of water on the phase-transfer properties of octan-1-ol. J. Chem. Soc. Perk. T. 2. 1992:2155–2161.
4. Sassi P, Paolantoni M, Cataliotti RS, Palombo F, Morresi A. Water/alcohol mixtures: A spectroscopic study of the water-saturated 1-octanol solution. J. Phys. Chem. B. 2004; 108:19557–19565.
5. Margolis SA, Levenson M. Certification by the Karl Fischer method of the water content in SRM 2890, water saturated 1-octanol, and the analysis of associated interlaboratory bias in the measurement process. Fresen. J. Anal. Chem. 2000; 367:1–7.
6. Franks NP, Abraham MH, Lieb WR. Molecular organization of liquid n-octanol: An X-ray diffraction analysis. J. Pharm. Sci. 1993; 82:466–470. [PubMed: 8360823]
7. Hu K, Zhou Y, Shen J, Ji Z, Cheng G. Microheterogeneous structure of 1-octanol in neat and water-saturated state. J. Phys. Chem. B. 2007; 111:10160–10165. [PubMed: 17683135]
8. MacCallum JL, Tieleman DP. Structures of neat and hydrated 1-octanol from computer simulations. J. Am. Chem. Soc. 2002; 124:15085–15093. [PubMed: 12475354]
9. Shallard-Brown HA, Watkin DJ, Cowley AR. n-Octanol. Acta Crystallogr. E. 2005; 61:213–214.
10. DeBolt SE, Kollman PA. Investigation of structure, dynamics, and solvation in 1-octanol and its water-saturated solution: Molecular dynamics and free-energy perturbation studies. J. Am. Chem. Soc. 1995; 117:5316–5340.
11. Balaz S. Lipophilicity in trans-bilayer transport and subcellular pharmacokinetics. Perspect. Drug Discov. Design. 2000; 19:157–177.

12. Seelig A, Gatlik-Landwojtowicz E. Inhibitors of multidrug efflux transporters: Their membrane and protein interactions. Mini0Rev. Med. Chem. 2005; 5:135–151.
13. Cojocaru V, Balali-Mood K, Sansom MSP, Wade RC. Structure and dynamics of the membrane-bound cytochrome P450 2C9. PLoS Comput. Biol. 2011; 7:e1002152. [PubMed: 21852944]
14. Luong C, Miller A, Barnett J, Chow J, Ramesha C, Browner MF. Flexibility of the NSAID binding site in the structure of human cyclooxygenase-2. Nat. Struct. Biol. 1996; 3:927–933. [PubMed: 8901870]
15. Marrink SJ, Berendsen HJC. Simulation of water transport through a lipid membrane. J. Phys. Chem. 1994; 98:4155–4168.
16. Scheuplein RJ, Blank IH, Brauner GJ, MacFarlane DJ. Percutaneous absorption of steroids. J. Invest. Dermatol. 1969; 52:63–70. [PubMed: 5761930]
17. Riebesehl W, Tomlinson E, Gruenbauer HJM. Thermodynamics of solute transfer between alkanes and water. J. Phys. Chem. 1984; 88:4775–4779.
18. Schulte J, Durr J, Ritter S, Hauthal WH, Quitzsch K, Maurer G. Partition coefficients for environmentally important, multifunctional organic compounds in hexane + water. J. Chem. Eng. Data. 1998; 43:69–73.
19. Runyan A, Perrin JH, Vilallonga FA. Interfacial tensions and partition coefficients in water/heptane systems containing 2,6-diisopropylphenol, n-alkylphenols and cycloalkanols. J. Pharm. Pharmacol. 1988; 40:203–204. [PubMed: 2899151]
20. Chikhale EG, Ng KY, Burton PS, Borchardt RT. Hydrogen bonding potential as a determinant of the in vitro and in situ blood-brain barrier permeability of peptides. Pharm Res. 1994; 11:412–419. [PubMed: 8008709]
21. Xiang TX, Anderson BD. The relationship between permeant size and permeability in lipid bilayer membranes. J. Membrane Biol. 1994; 140:111–122. [PubMed: 7932645]
22. Abraham MH, Acree WE Jr. Leo AJ, Hoekman D, Cavanaugh JE. Water-solvent partition coefficients and ΔLog P values as predictors for blood-brain distribution; application of the Akaike information criterion. J. Pharm. Sci. 2010; 99:2492–2501. [PubMed: 19967782]
23. Hafkenscheid TL, Tomlinson E. Correlations between alkane/water and 1-octanol/water distribution coefficients and isocratic reversed-phase liquid chromatographic capacity factors of acids, bases and neutrals. Int. J. Pharmaceutics. 1983; 16:225–239.
24. Young RC, Mitchell RC, Brown TH, Ganellin CR, Griffiths R, Jones M, Rana KK, Saundners DD, Smith IR, Sore NE, Wilks TJ. Development of a new physicochemical model for brain penetration and its application to the design of centrally acting H2 receptor histamine antagonists. J. Med. Chem. 1988; 31:656–671. [PubMed: 2894467]
25. van de Waterbeemd H, Kansy M. Hydrogen-bonding capacity and brain penetration. Chimia. 1992; 46:299–303.
26. Caron G, Ermondi G. Calculating virtual log P in the alkane/water system (log P^{N}_{alk}) and its derived parameters Δlog $P^{N}_{oct\text{-}alk}$ and log D^{pH}_{alk}. J. Med. Chem. 2005; 48:3269–3279. [PubMed: 15857133]
27. Barry JA, Gawrisch K. Direct NMR evidence for ethanol binding to the lipid-water interface of phospholipid bilayers. Biochemistry. 1994; 33:8082–8088. [PubMed: 8025114]
28. Balgavy P, Dubnickova M, Kucerka N, Kiselev MA, Yaradaikin SP, Uhrikova D. Bilayer thickness and lipid interface area in unilamellar extruded 1,2-diacylphosphatidylcholine liposomes: A small-angle neutron scattering study. Biochim. Biophys. Acta. 2001; 1512:40–52. [PubMed: 11334623]
29. Hristova K, White SH. Determination of the hydrocarbon core structure of fluid dioleoylphosphocholine (DOPC) bilayers by X-ray diffraction using specific bromination of the double-bonds: Effect of hydration. Biophys. J. 1998; 74:2419–2433. [PubMed: 9591668]
30. Eisenberg D, Weiss RM, Terwilliger TC. The helical hydrophobic moment: A measure of the amphiphilicity of a helix. Nature. 1982; 299:371–374. [PubMed: 7110359]
31. Brasseur R, Vandenbosch C, van den Bossche H, Ruysschaert J-M. Mode of inserion of miconazole ketonazole and deacylated ketoconazole in lipid layers. A conformational analysis. Biochem. Pharmacol. 1983; 32:2175–2180. [PubMed: 6307314]

32. Fischer H, Kansy M, Bur D. CAFCA: A novel tool for the calculation of amphiphilic properties of charged drug molecules. Chimia. 2000; 54:640–645.
33. Kessel A, Musafia B, Ben-Tal N. Continuum solvent model studies of the interactions of an anticonvulsant drug with a lipid bilayer. Biophys. J. 2001; 80:2536–2545. [PubMed: 11371432]
34. Oren I, Fleishman SJ, Kessel A, Ben Tal N. Free diffusion of steroid hormones across biomembranes: A simplex search with implicit solvent model calculations. Biophys. J. 2004; 87:768–779. [PubMed: 15298886]
35. Tanaka M, Fukuda H, Nagai T. Permeation of drug through a model membrane consisting of millipore filter with oil. Chem. Pharm. Bull. 1978; 26:9–13.
36. Leahy DE, Taylor PJ, Wait AR. Model solvent systems for QSAR. 1. Propylene glycol dipelargonate (PGDP). A new standard solvent for use in partition coefficient determination. Quant. Struct.0Act. Relat. 1989; 8:17–31.
37. el-Tayar N, Tsai RS, Testa B, Carrupt PA, Hansch C, Leo A. Percutaneous penetration of drugs: A quantitative structure-permeability relationship study. J. Pharm. Sci. 1991; 80:744–749. [PubMed: 1791533]
38. Seiler P. Interconversion of lipophilicities from hydrocarbon/water systems into the octanol/water system. Eur. J. Med. Chem. 1974; 9:473–479.
39. Lukacova V, Peng M, Tandlich R, Hinderliter A, Balaz S. Partitioning of organic compounds in phases imitating the headgroup and core regions of phospholipid bilayers. Langmuir. 2006; 22:1869–1874. [PubMed: 16460120]
40. Kakemi K, Sezaki H, Muranishi S, Tsujimura Y. Absorption and excretion of drugs. XL. Enhancement of the rectal absorption of pharmaceutical amines with lauryl sulfate and saccharinate anions. Chem. Pharm. Bull. 1969; 17:1641–1650. [PubMed: 5348892]
41. Weilgung F. The local stimulating effect of calcium salts in relation to their chemical constitution. Arch. Exp. Pathol. Pharmakol. 1932; 167:71–72.
42. Burton PS, Conradi RA, Hilgers AR, Ho NFH, Maggiora LL. The relationship between peptide structure and transport across epithelial cell monolayers. J. Control. Release. 1992; 19:87–97.
43. Niimi AJ. Solubility of organic chemicals in octanol, triolein and cod liver oil and relationships between solubility and partition coefficients. Water Res. 1991; 25:1515–1521.
44. Poulin P, Krishnan K. A biologically-based algorithm for predicting human tissue:blood partition coefficients of organic chemicals. Human Exp.Ttoxicol. 1995; 14:273–280.
45. Poulin P, Krishnan K. Molecular structure-based prediction of the partition coefficients of organic chemicals for physiological pharmacokinetic models. Toxicol. Meth. 1996; 6:117–137.
46. Poulin P, Theil FP. A priori prediction of tissue:plasma partition coefficients of drugs to facilitate the use of physiologically-based pharmacokinetic models in drug discovery. J. Pharm. Sci. 2000; 89:16–35. [PubMed: 10664535]
47. Mannhold R, van de Waterbeemd H. Substructure and whole molecule approaches for calculating log P. J. Comp. Aid. Mol. Des. 2001; 15:337–354.
48. Zerara M, Brickmann J, Kretschmer R, Exner TE. Parameterization of an empirical model for the prediction of n-octanol, alkane and cyclohexane/water as well as brain/blood partition coefficients. J. Comput. -Aided Mol. Des. 2009; 23:105–111. [PubMed: 18818882]
49. Abraham MH, Acree WE. Linear free-energy relationships for water/hexadec-1-ene and water/deca-1,9-diene partitions, and for permeation through lipid bilayers; comparison of permeation systems. New J. Chem. 2012; 36:1798–1806.
50. Nitsche JM, Kasting GB. A correlation for 1,9-decadiene/water partition coefficients. J. Pharm. Sci. 2013; 102:136–144. [PubMed: 23132301]
51. Leo A, Jow PY, Silipo C, Hansch C. Calculation of hydrophobic constant (log P) from π and f constants. J. Med. Chem. 1975; 18:865–868. [PubMed: 1159707]
52. Origin 7.0. Origin Lab; Northampton, MA: 2002.
53. Abraham MH, Chadha HS, Whiting GS, Mitchell RC. Hydrogen bonding. 32. An analysis of water-octanol and water-alkane partitioning and the delta log P parameter of Seiler. J. Pharm. Sci. 1994; 83:1085–1100. [PubMed: 7983591]

54. Avdeef A. pH-metric log P. Part 1. Difference plots for determining ion-pair octanol-water partition coefficients of multiprotic substances. Quant. Struct.0Act. Rel. 1992; 11:510–517.
55. Box, K.; Comer, J.; Huque, F. Pharmacokinetic Profiling in Drug Research. Wiley-VCH Verlag; 2006. Correlations between PAMPA permeability and log P; p. 243-257.
56. Caron G, Carrupt PA, Testa B, Ermondi G, Gasco A. Insight into the lipophilicity of the aromatic N-oxide moiety. Pharm. Res. 1996; 13:1186–1190. [PubMed: 8865309]
57. Caron G, Gaillard P, Carrupt PA, Testa B. Lipophilicity behavior of model and medicinal compounds containing a sulfide, sulfoxide, or sulfone moiety. Helv. Chim. Acta. 1997; 80:449–462.
58. el Tayar N, Tsai RS, Testa B, Carrupt PA, Leo A. Partitioning of solutes in different solvent systems. The contribution of hydrogen-bonding capacity and polarity. J. Pharm. Sci. 1991; 80:590–598. [PubMed: 1941553]
59. Gobas FAPC, Lahittete JM, Garofalo G, Shiu WY, Mackay D. A novel method for measuring membrane-water partition coefficients of hydrophobic organic chemicals: Comparison with 1-octanol-water partitioning. J. Pharm. Sci. 1988; 77:265–272. [PubMed: 3373432]
60. Hansch, C.; Leo, A. Substituent Constants for Correlation Analysis in Chemistry and Biology. Wiley; New York: 1979.
61. Leahy DE, Morris JJ, Taylor PJ, Wait AR. Model solvent systems for QSAR 2. Fragment values ('f-values') for the 'critical quartet'. J. Chem. Soc. Perk. T. 2. 1992:723–731.
62. Lukacova V, Peng M, Fanucci G, Tandlich R, Hinderliter A, Maity B, Mannivanan E, Cook GR, Balaz S. Drug-membrane interactions studied in phospholipid monolayers adsorbed on nonporous alkylated microspheres. J. Biomol. Screen. 2007; 12:186–202. [PubMed: 17218665]
63. Pagliara A, Testa B, Carrupt PA, Jolliet P, Morin C, Morin D, Urien S, Tillement JP, Rihoux JP. Molecular properties and pharmacokinetic behavior of cetirizine, a zwitterionic H1-receptor antagonist. J. Med. Chem. 1998; 41:853–863. [PubMed: 9526560]
64. Ter Laak AM, Tsai RS, Donne-Op den Kelder GM, Carrupt PA, Testa B, Timmerman H. Lipophilicity and hydrogen-bonding capacity of H1-antihistaminic agents in relation to their central sedative side-effects. Eur. J. Pharm. Sci. 1994; 2:373–384.
65. ClogP version 3.51. Daylight Chemical Information Systems; Irvine, CA: 1991.
66. Toulmin A, Wood JM, Kenny PW. Toward prediction of alkane/water partition coefficients. J. Med. Chem. 2008; 51:3720–3730. [PubMed: 18558667]
67. Wohnsland F, Faller B. High-throughput permeability pH profile and high-throughput alkane/water log P with artificial membranes. J. Med. Chem. 2001; 44:923–930. [PubMed: 11300874]
68. Bio-Loom for Windows version 1.5. BioByte Corp.; Claremont, CA: 2006.
69. SAS Enterprise Guide version 4.3. SAS Institute Inc; Cary, NC: 2010.
70. Kubinyi H. Drug partitioning: Relationships between forward and reverse rate constants and partition coefficient. J. Pharm. Sci. 1978; 67:262–263. [PubMed: 621652]
71. van de Waterbeemd H, van Bakel H, Jansen A. Transport in quantitative structure-activity relationships VI: Relationship between transport rate constants and partition coefficients. J. Pharm. Sci. 1981; 70:1081–1082. [PubMed: 6101160]
72. Balaz S. Modeling kinetics of subcellular disposition of chemicals. Chem. Rev. 2009; 109:1793–1899. [PubMed: 19265398]
73. de Bruijn J, Busser F, Seinen W, Hermens J. Determination of octanol/water partition coefficients for hydrophobic organic chemicals with the "slow-stirring" method. Environ. Toxicol. Chem. 1989; 8:499–512.
74. Leo A. The octanol-water partition coefficient of aromatic solutes: The effect of electronic interactions, alkyl chains, hydrogen bonds, and ortho-substitution. J. Chem. Soc. Perk. T. 2. 1983:825–838.
75. Platts JA, Butina D, Abraham MH, Hersey A. Estimation of molecular linear free energy relation descriptors using a group contribution approach. J. Chem. Inf. Comp. Sci. 1999; 39:835–845.
76. Abraham MH, Platts JA. Hydrogen bond structural group constants. J. Org. Chem. 2001; 66:3484–3491. [PubMed: 11348133]

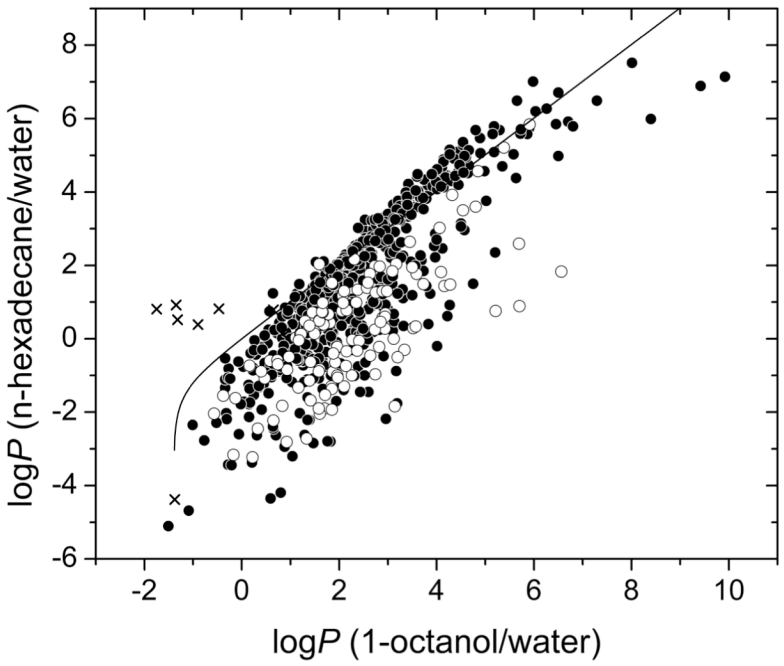

Figure 1.

The plot of n-hexadecane/water and 1-octanol/water partition coefficients for 693 studied compounds: neutral compounds (full points), fully or partially ionizable molecules (open points), and small molecules such as gases and water (crosses). The straight portion of the line is close to the identity line. The curvature indicates the hypothetical limitation of the $P_{O/W}$ value for hydrophilic compounds by the high water content of 1-octanol. See text for more details.

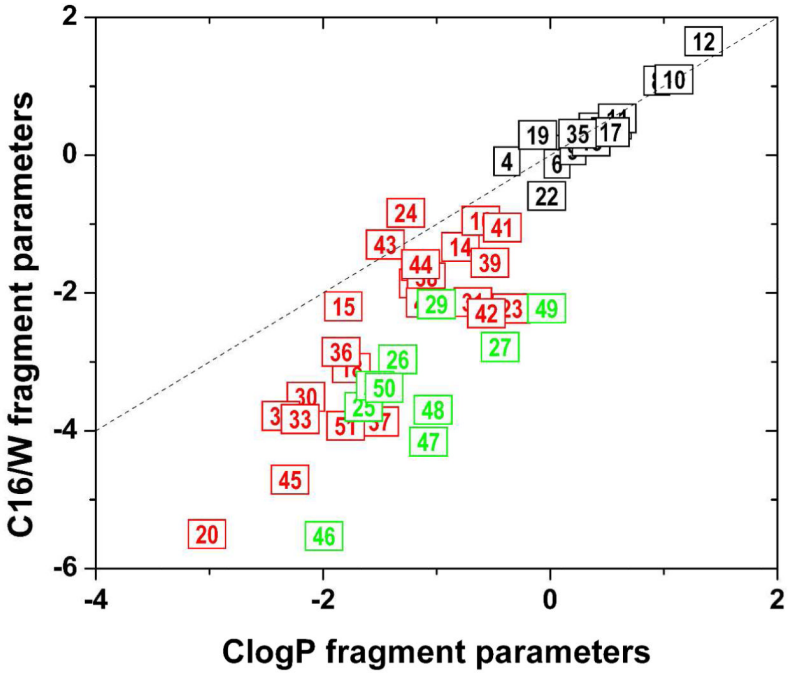

Figure 2.
Comparison of 1-hexadecane/water and 1-octanol/water (ClogP) fragment solvation parameters. The fragment numbers correspond to those in Table 2. The H-bond acceptors are shown in red and H-bond donors/acceptors are shown in green. The identity line is shown.

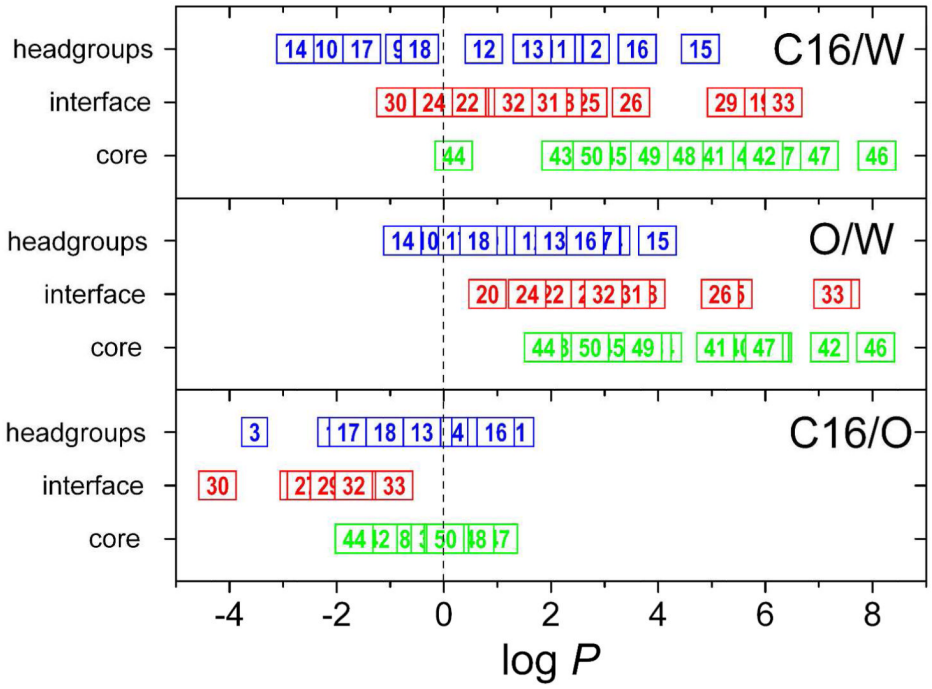

Figure 3.

Bilayer location for compounds partitioning primarily in headgroups (blue, numbers in Table 4), at the interface (red, numbers in Table 5), and in the core (green, numbers in Table 6) vs. the partition coefficients *P* in the shown two-phase systems: n-hexadecane/water (top panel), 1-octanol/water (middle panel), and n-hexadecane/1-octanol ($P_{C16/W}/P_{O/W}$, bottom panel).

Table 1

Measured n-Hexadecane/Water Partition Coefficients and Transport Rate Parameters

Compound	CAS Number	*P*	l_1 (cm/h)	l_2 (cm/h)
1,2-dimethoxybenzene	91-16-7	$(2.723\pm1.352)\times10^{1}$	1.171 ± 0.535	$(4.301\pm0.840)\times10^{-2}$
1-phenyl-1-propanol	93-54-9	3.153 ± 0.630	$(3.864\pm0.154)\times10^{-1}$	$(1.226\pm0.240)\times10^{-1}$
2-allylphenol [a]	1745-81-9	7.119 ± 3.070	$(2.286\pm0.857)\times10^{-1}$	$(3.211\pm0.685)\times10^{-2}$
2-phenylacetamide	103-84-4	$(5.861\pm2.227)\times10^{-2}$	$(1.624\pm0.359)\times10^{-2}$	$(2.771\pm0.857)\times10^{-1}$
2-phenylphenol [a]	90-43-7	$(3.536\pm1.329)\times10^{1}$	$(3.699\pm0.935)\times10^{-1}$	$(1.046\pm0.291)\times10^{-2}$
3-bromoaniline	591-19-5	$(1.107\pm0.106)\times10^{1}$	$(6.304\pm0.471)\times10^{-1}$	$(5.693\pm0.339)\times10^{-2}$
4-bromobenzophenone	90-90-4	$(2.891\pm0.684)\times10^{2}$	$(1.054\pm0.026)\times10^{1}$	$(3.646\pm0.858)\times10^{-2}$
4-bromophenol	106-41-2	$(9.700\pm3.925)\times10^{-1}$	$(2.054\pm0.524)\times10^{-1}$	$(2.118\pm0.665)\times10^{-1}$
4-chloro-2-nitrotoluene	89-59-8	$(8.660\pm3.938)\times10^{2}$	$(2.168\pm0.605)\times10^{2}$	$(2.504\pm0.899)\times10^{-1}$
4-chloro-3-methylphenol	59-50-7	1.651 ± 0.701	$(1.491\pm0.611)\times10^{-1}$	$(9.029\pm1.001)\times10^{-2}$
4-chlorobenzophenone	134-85-0	$(7.315\pm2.674)\times10^{2}$	$(1.102\pm0.216)\times10^{2}$	$(1.507\pm0.465)\times10^{-1}$
4-nitroaniline	100-01-6	$(1.890\pm0.656)\times10^{-1}$	$(1.192\pm0.406)\times10^{-1}$	$(6.295\pm0.407)\times10^{-1}$
9-anthracenemethanol [a]	1468-95-7	$(2.211\pm0.554)\times10^{2}$	1.565 ± 0.236	$(7.080\pm1.416)\times10^{-3}$
acetanilide	103-84-4	$(2.580\pm0.857)\times10^{-1}$	$(1.315\pm0.434)\times10^{-1}$	$(5.104\pm0.179)\times10^{-1}$
aniline	62-53-3	$(7.860\pm1.639)\times10^{-1}$	$(1.502\pm0.286)\times10^{-1}$	$(1.912\pm0.162)\times10^{-1}$
benzocaine [a]	94-09-7	1.560 ± 0.666	$(1.163\pm0.488)\times10^{-1}$	$(7.455\pm0.577)\times10^{-2}$
caffeine	58-08-2	$(2.376\pm0.576)\times10^{-1}$	$(5.485\pm0.851)\times10^{-2}$	$(2.309\pm0.430)\times10^{-1}$
ethylnicotinate	614-18-6	3.583 ± 0.983	$(5.074\pm1.031)\times10^{-1}$	$(1.416\pm0.261)\times10^{-1}$
formanilide	103-70-8	$2.900\pm0.955)\times10^{-1}$	$(1.532\pm0.501)\times10^{-1}$	$(5.283\pm0.213)\times10^{-1}$
indole	120-72-9	5.660 ± 0.633	$(6.291\pm0.522)\times10^{-1}$	$(1.111\pm0.083)\times10^{-1}$
nifedipine	21829-25-4	4.827 ± 2.241	$(7.229\pm2.679)\times10^{-1}$	$(1.498\pm0.418)\times10^{-1}$
nitrobenzene	98-95-3	$(2.942\pm0.756)\times10^{1}$	1.162 ± 0.218	$(3.950\pm0.694)\times10^{-2}$
N-methylbenzamide	613-93-4	$(6.450\pm1.180)\times10^{-1}$	$(4.982\pm0.860)\times10^{-1}$	$(7.724\pm0.467)\times10^{-1}$
pyridine	110-86-1	$(3.560\pm1.562)\times10^{-1}$	$(9.512\pm0.343)\times10^{-2}$	$(2.672\pm0.669)\times10^{-1}$
quinoline	91-22-5	$(1.056\pm0.360)\times10^{1}$	$(3.766\pm0.198)\times10^{-1}$	$(3.566\pm1.200)\times10^{-2}$

[a] this value supersedes the published value[62]

J Chem Inf Model. Author manuscript; available in PMC 2014 June 24.

Table 2

Fragment Solvation Parameters, *f*, in the n-Hexadecane/Water System

Fragment			Solvation Parameters		Contributions to Solvatochromic Parameters [a]					Count [d]
No.	**Description** [b]	**Symbol**	**O/W** [c]	**C16/W**	***E***	***S***	***A***	***B***	***V***	
1	hydrogen on isolating carbon	H	0.227	0.287±0.020	–	–	0	0	–	508
2	aliphatic [A] isolating carbon	CA	0.195	0.108±0.060	0	0	0	0	0.1409	413
3	aromatic [a] isolating carbon	Ca	0.13	0.077±0.021	0	0	0	0	0.1194	251
4	fluoride [A]	FA	−0.38	−0.090±0.076	0.08	0.350	0	0.1	0.1262	3
5	fluoride [a]	Fa	0.37	0.399±0.092	–	–	0	−0.04	–	7
6	chloride [A]	ClA	0.06	−0.126±0.047	0.271	0.400	0	0.1	0.2310	30
7	chloride [V]	ClV	0.60	0.442±0.058	–	–	–	–	–	6
8	chloride [a]	Cla	0.94	1.078±0.045	–	–	0	−0.07	–	41
9	bromide [A]	BrA	0.20	0.069±0.053	0.432	0.400	0	0.12	0.2836	18
10	bromide [a]	Bra	1.09	1.096±0.044	–	–	0	−0.05	–	13
11	iodide [A]	IA	0.59	0.532±0.109	0.712	0.400	0	0.15	0.3668	6
12	iodide [a]	Ia	1.35	1.651±0.165	–	–	0	−0.02	–	3
13	sulfur in aromatic ring [aa]	Saraa	0.36	0.198±0.137	–	–	–	–	–	4
14	sulfide [AA] [e]	SAA	−0.79	−1.334±0.125	0.435	0.380	0	0.32	0.2721	5
15	ether [AA] [e]	OAA	−1.82	−2.197±0.115	0.041	0.250	0	0.45	0.1673	7
16	ether [Aa] [e]	OAa	−0.61	−0.955±0.084	–	–	0	0.18	–	19
17	ether [aa]	Oaa	0.53	0.332±0.086	–	–	–	–	–	4
18	oxygen in aliphatic ring [RR] [e]	ORR	−1.75	−3.091±0.123	0.261	0.490	0	0.48	0.0587	6
19	oxygen in aromate [aa]	Oxgenaa	−0.11	0.292±0.160	–	–	–	–	–	3
20	N-oxide with N in aromate [aa] [e]	Noxide	−3.02	−5.503±0.138	–	–	–	–	–	4
21	nitro [A] [e]	NO2A	−1.16	−1.864±0.101	0.356	0.950	0	0.31	0.2828	7
22	nitro [a]	NO2a	−0.03	−0.592±0.097	–	–	0	0.14	–	12
23	nitrile [A] [e]	CNA	−0.34	−2.229±0.119	0.312	0.900	0	0.36	0.2633	5

Fragment			Solvation Parameters		Contributions to Solvatochromic Parameters [a]					Count [d]
No.	Description [b]	Symbol	O/W [c]	C16/W	*E*	*S*	*A*	*B*	*V*	
24	nitrile [a] [e]	CNa	−1.27	−0.873±0.140	–	–	0	0.19	–	4
25	hydroxyl [A] [f]	OHA	−1.64	−3.656±0.053	0.31	0.420	0.37	0.48	0.1673	48
26	hydroxyl [Z] [f]	OHZ	−1.34	−2.967±0.101	–	–	–	–	–	10
27	hydroxyl [a] [f]	OHa	−0.44	−2.788±0.053	–	–	0.6	0.16	–	46
28	primary amine [A] [f]	NH2A	−1.54	−3.349±0.076	0.264	0.350	0.16	0.61	0.2084	14
29	primary amine [a] [f]	NH2a	−1.00	−2.166±0.072	–	–	0.26	0.27	–	34
30	secondary amine [AA] [e]	NHAA	−2.15	−3.509±0.109	0.224	0.300	0.08	0.69	0.2084	9
31	NH in aromatic ring [e]	NHaa	−0.68	−2.136±0.158	–	–	–	–	–	3
32	tertiary amine [AAA] [e]	NAAA	−2.37	−3.786±0.112	0.179	0.150	0	0.79	0.2084	8
33	nitrogen in aliphatic ring [RR] [e]	NARR	−2.20	−3.830±0.178	0.342	0.460	0.13	0.68	0.0998	3
34	nitrogen in aromatic ring [aa] [e]	Naraa	−1.14	−1.611±0.077	–	–	–	–	–	21
35	trifluoromethyl [A] or [a]	CF3Aa	0.24	0.310±0.126	−0.3	0.100	0	−0.03	0.3023	5
36	carbonyl [AA] [e]	COAA	−1.84	−2.857±0.073	0.204	0.660	0	0.51	0.2652	24
37	carbonyl [RW] [e]	CORW	−1.50	−3.866±0.251	–	–	–	–	–	7
38	carbonyl [Aa] [e]	COAa	−1.09	−1.774±0.097	–	–	0	0.37	–	11
39	carbonyl [aa] [e]	COaa	−0.53	−1.562±0.178	–	–	–	–	–	3
40	aldehyde [A] [e]	ALA	−1.1	−2.144±0.084	0.222	0.650	0	0.45	0.2652	11
41	aldehyde [a] [e]	ALa	−0.42	−1.052±0.103	–	–	0	0.25	–	9
42	ester [AA] [e]	EsAA	−0.56	−2.298±0.068	0.197	0.580	0	0.45	0.3239	21
43	ester [Aa] [e]	EsAa	−1.45	−1.299±0.105	–	–	0	0.32	–	17
44	formyl ester [A] [e]	EsFA	−1.14	−1.585±0.108	0.238	0.660	0	0.38	0.3239	6
45	phosphate ester [AAA] [e]	EsPAAA	−2.29	−4.710±0.449	0.226	1.000	0	1.06	0.5480	4

Fragment			Solvation Parameters		Contributions to Solvatochromic Parameters [a]					Count [d]
No.	Description [b]	Symbol	O/W [c]	C16/W	*E*	*S*	*A*	*B*	*V*	
46	amide [A] [f]	AmideA	−1.99	−5.531±0.133	0.48	1.300	0.55	0.68	0.3650	4
47	carboxyl [A] [f]	COOHA	−1.07	−4.161±0.088	0.297	0.650	0.6	0.45	0.3239	11
48	carboxyl [Z] [f]	COOHZ	−1.03	−3.697±0.134	–	–	0.6	0.47	–	5
49	carboxyl [a] [f]	COOHa	−0.03	−2.228±0.120	–	–	0.59	0.26	–	6
50	carbamate [Aa] [f]	CBMTAa	−1.46	−3.378±0.123	–	–	0.36	0.41	–	5
51	carbamate with N in ring [RRa] [e]	CBMTRRa	−1.80	−3.928±0.166	–	–	–	–	–	3

[a] fragment contributions to excess molar refraction *E*, dipolarity/polarizability *S*, overall H-bond acidity *A*, overall H-bond basicity *B*, and volume V estimed as described in the text

[b] attached to A – aliphatic, a – aromatic, V – vinyl, Z – benzyl structure or inside the ring(s) RR – aliphatic, RW – aliphatic with a conjugated double bond

[c] 1-octanol/water fragment values are shown for comparison

[d] the number of compounds in which the given fragment is encountered

[e] H-bond acceptors

[f] H-bond donors and acceptors (see text for classification criteria).

Table 3

Correction Factors, *F*, in the n-Hexadecane/Water System

No.	Description	Symbol	Parameter Estimates with Standard Error		Count[b]
			O/W[a]	C16/W	
52	alicyclic	Alicyclic	−0.09	−0.033±0.031	45
53	benzyl bond to simple aromatics	BB	−0.15	−0.177 ±0.041	93
54	double bond	Bond2	−0.03	−0.039±0.074	28
55	triple bond	Bond3	−0.45	−0.595±0.136	6
56	non-halogen, polar group branch	BranchP	−0.22	−0.089±0.046	51
57	chain	Chain	−0.12	−0.057±0.030	329
58	chain and cluster branch	ChBr	−0.13	−0.125±0.025	80
59	extended aromatic iso-carbon	FAC	0.10	0.149±0.039	52
60	interacting F and non-F fragments	FnonF	0.28	0.246±0.055	9
61	proximity -fragments YCY	FragYCY	1.12 to 1.46	2.165±0.120	6
62	pair - H bond	HB	0.07 to 1.00	1.323±0.119	6
63	interacting fragments (halogens)	InterFrag	0.3,0.53, 0.7	0.485±0.044	22
64	net bond counts (fragbranch)	NetBond	−0.28	−0.187±0.101	4
65	ortho substitution 1	NOrthol	MV [c]	0.147±0.058	24
66	ortho substitution 2	NOrtho2		−0.476±0.058	18
67	ortho substitution 3	NOrtho3		−0.270±0.073	8
68	ether in a 5-membered ring	O5R	0.13, 0.57	0.414±0.186	3
69	phenyl-fragment pair	PCCY	0.15	0.244±0.103	10
70	potential interaction within ring 1	PIWR1	MV [c]	0.092±0.072	16
71	potential interaction within ring 2	PIWR2		0.114±0.060	37
72	potential interaction within ring 3	PIWR3		0.370±0.119	16
73	pair -proximity	Proximity	0.28 to 0.907	1.207±0.088	11
74	11-hydroxy non-dienyl steroid	Steroid	1.16	1.912±0.200	3
75	extra benzyl (class Ortho)	XBenzyl	−0.40 to −0.05	0.333±0.146	4
76	Y-fragment	Yfragment	0.4, 0.9, 1.3	0.607±0.119	7

[a] the 1-octanol/water values are shown for comparison

[b] the number of compounds in which the given fragment is encountered

[c] multiple values – discussed in the text

Table 4

Partition Coefficients of Cephalophiles Locating in Headgroup Stratum[72]

No.	Compound	log*P*		
		C16/W[a]	O/W[b]	C16/O[c]
1	1-chloro-1,2,2-trifluorocyclobutane	3.726[a]	2.290[b]	1.436
2	1H-indene	2.842[a]	2.920	−0.078
3	1H-indole-3-butanoic acid	−1.721a	1.810[b]	−3.531
4	2-[4-N(CHs)2-phenyl]-3-OH-flavone	3.494[a]	3.230[b]	0.264
5	3-methylindole	0.810	2.170[b]	−1.360
6	9H-carbazole	2.209[a]	3.060[b]	−0.851
7	9-hydroxymethylanthracene	2.340	3.040	−0.700
8	benzylalcohol	−0.430	1.100	−1.530
9	ephedrine	−0.840	0.930	−1.770
10	ethanol	−2.190	−0.310	−1.880
11	halothane	2.100	2.300	−0.200
12	indole	0.750	1.670[b]	−0.920
13	isofluorane	1.650	2.060	−0.410
14	methanol	−2.770	−0.770	−2.000
15	N-methylcarbazole	4.789[a]	3.990	0.799
16	N-methylindole	3.609[a]	2.640	0.969
17	propanol	−1.530	0.250	−1.780
18	pyridine	−0.450	0.650	−1.100

[a]predicted using the fragments and factors in Tables 2 and 3, 95% confidence intervals for the predicted values are shown in Supporting Information Table S3, the remaining values are measured and listed in Table S1 in Supporting Information

[b]ClogP predictions, the remaining values are listed in the ClogP database

[c]Calculated as log$P_{C16/W}$-log$P_{O/W}$

Table 5

Partition Coefficients of Amphiphiles Locating at the Interface[72]

No.	Compound	log*P*		
		C16/W[a]	O/W[b]	C16/O[c]
19	11-(9-carbazole)-undecanoic acid	5.912[a]	7.330[b]	−1.418
20	1-butanol	−0.811[a]	0.880	−1.631
21	1-heptanol	1.065[a]	2.720	−1.655
22	1-hexanol	0.440[a]	2.030	−1.590
23	1-octanol	1.690[a]	3.000	−1.310
24	1-pentanol	−0.185[a]	1.560	−1.745
25	4-(6-phenyl-1,3,5-hexatrien-1-yl)-benzenepropanoic acid	2.698[a]	5.400[b]	−2.702
26	4-tert-octylphenol	3.495[a]	5.160[b]	−1.665
27	9-anthracene-acetic acid	1.190[a]	3.760[b]	−2.570
28	9-anthracene-ethanamine	2.231[a]	3.780[b]	−1.549
29	Δ8-tetrahydrocannabinol	5.271[a]	7.410	−2.139
30	bisphenol A	−0.902	3.320	−4.222
31	ibuprofen	1.950	3.500	−1.550
32	propranolol	1.300	2.980	−1.680
33	totarol	6.336[a]	7.260[b]	−0.924

[a] predicted using the fragments and factors in Tables 2 and 3, 95% confidence intervals for the predicted values are shown in Supporting Information Table S3, the remaining values are measured and listed in Table S1 in Supporting Information

[b] ClogP predictions, the remaining values are listed in the ClogP database

[c] Calculated as log$P_{C16/W}$-log$P_{O/W}$

Table 6

Partition Coefficients of Lipophiles Locating in the Core[72]

No.	Compound[a]	logP		
		C16/W[a]	O/W[b]	C16/O[c]
34	1,2-dichlorohexafluorocyclobutane	4.198[a]	4.090[b]	0.108
35	1,4-dimethylbenzene	3.250	3.150	0.100
36	1,6-diphenyl-1,3,5-hexatriene	5.828[a]	5.640[b]	0.188
37	1-methyl-4-(6-phenyl-1,3,5-hexatrien-1-yl)-benzene	6.333[a]	6.140[b]	0.193
38	4-bromo-2,6-*t*-butyl-phenol	5.257[a]	6.090[b]	−0.833
39	4-methyl-2,6-*t*-butyl-phenol	4.840[a]	5.100	−0.260
40	9-ethyl anthracene	5.680[a]	5.520[b]	0.160
41	9-methylanthracene	5.055[a]	5.070	−0.015
42	amiodarone	5.981[a]	7.200[b]	−1.219
43	benzene	2.150	2.130	0.050
44	benzocaine	0.190	1.860	−1.670
45	ethylbenzene	3.200	3.150	0.050
46	methoxy-Δ8-tetrahydrocannabinol	8.087[a]	8.060	0.027
47	n-decane	7.010	5.980[b]	1.030
48	n-hexane	4.490	3.900	0.590
49	n-propylbenzene	3.840	3.720	0.120
50	toluene	2.760	2.730	0.030

[a] β-carotene, canthaxanthin, lutein, squalene, and zeaxanthin were not used because of unreliable logP predictions

[b] partition coefficients predicted using the fragments and factors in Tables 2 and 3, 95% confidence intervals for the predicted values are shown in Supporting Information Table S3, the remaining values are measured and listed in Table S1 in Supporting Information; [b] ClogP predictions, the remaining values are listed in the ClogP database

[c] Calculated as $\log P_{C16/W} - \log P_{O/W}$